JOURNAL OF PROPULSION AND POWER
Vol. 23, No. 2, March–April 2007

Solid Propellant Grain Design and Burnback Simulation Using a Minimum Distance Function

Michael A. Willcox,* M. Quinn Brewster,† K. C. Tang,‡ and D. Scott Stewart§
University of Illinois at Urbana–Champaign, Urbana, Illinois 61801

DOI: 10.2514/1.22937

A fast computational method for simulating the evolution of the burning surface of a complex, three-dimensional solid rocket motor propellant grain has been developed using a signed minimum distance function. The minimum distance function is calculated using stereo-lithography surface information from a computer-aided-design file and propellant surface burnback is simulated by manipulation of the initial minimum distance function. Variable time stepping and multiple spatial grids further reduce computation time requirements. Results indicate that this method gives adequate accuracy with acceptable computation time for time scales of the full motor burn. The resulting code (Rocgrain) allows for motor grain design by user-friendly commercial computer-aided-design programs and for coupling with internal flow codes. This enables a single geometric tool to be used for describing the propellant grain geometry for both grain design and internal flowfield analysis. The Rocgrain code can be coupled with a variety of flowfield codes ranging in complexity from simple zero-dimensional to more sophisticated computational fluid dynamics analysis (e.g., nonlinear acoustic instability).

Nomenclature

a_x, a_y, a_z	=	coordinates of vertex of a triangle
d	=	distance from a point to a plane
d_b	=	burnt distance
N	=	number of grids or number of triangles
$\boldsymbol{n}$	=	unit normal vector
n_x, n_y, n_z	=	component of unit normal vector $\boldsymbol{n}$ in the x-, y-, or z-direction
P	=	perimeter
r_b	=	burning rate
t	=	time
x, y, z	=	Cartesian coordinates
Δt	=	time step
θ	=	angle between two adjacent triangles

Subscripts

A, B, C	=	vertices of a triangle
b	=	burnt
i, j, k	=	index in x-, y-, or z-direction
max	=	maximum
min	=	minimum
s	=	surface
x, y, z	=	Cartesian coordinate directions

Presented as Paper 4350 at the 41st AIAA/ASME/SAE/ASEE Joint Propulsion Conference & Exhibit, Tucson, AZ, 10–13 July 2005; received 3 February 2006; revision received 5 July 2006; accepted for publication 18 August 2006.

*Research Assistant, Department of Mechanical Science and Engineering, 1206 West Green Street. Member AIAA.

†Hermia G. Soo Professor, Department of Mechanical Science and Engineering, 1206 West Green Street. Fellow AIAA.

‡Research Scientist, Department of Mechanical Science and Engineering, 1206 West Green Street. Member AIAA.

§Professor, Department of Mechanical Science and Engineering, 1206 West Green Street. Associate Fellow AIAA.

I. Introduction

BURNING of solid propellant (SP) is mostly unsteady due to the changes in burning environment in response to transient events such as initial pressurization, combustion instability, and tail-off. Because pressure and flow conditions are not uniform in a solid rocket motor (SRM), solid propellant also rarely burns uniformly. The pressure drop inside a chamber causes the propellant to burn faster at head-end due to higher local pressure. Meanwhile, the effect of erosive burning enhances the burning rate toward the aft-end as the distance from head-end increases. Acoustic combustion instability, which depends on the solid propellant grain and chamber geometry, can change the local burning rate through fluctuations in local pressure and flowfield. These competing factors greatly influence the geometry of the solid propellant grain and the performance of an SRM during the burn. The highly nonuniform burning of propellant can significantly affect the characteristics of an SRM at initial pressurization [1,2], at intermediate "quasi-steady" conditions (through acoustic motions), and at tail-off [2]. The capability to model the instantaneous geometry of a solid propellant grain during the burnout of the entire grain is crucial to predicting the internal ballistics of an SRM.

There are a variety of ways to numerically represent the geometric information that defines a two- or three-dimensional solid and its surface. One of these methods is the level set method [3] and has been used in describing the burnback of solid propellant grain [4]. The level set method embeds the interface as the zero level set of the signed distance function to track the motion of an interface. The evolution of the zero level set of the level set function represents the motion of the interface, and the resulting initial value partial differential equation (PDE) for the evolution of the level set function resembles a Hamilton–Jacobi equation. This hyperbolic PDE equation is solved using entropy-satisfying schemes borrowed from the numerical solution of hyperbolic conservation laws, which produce the correct viscosity solution. The level set method allows easy evaluation of the curvatures and normals, and natural evolution of topology.

Another way to describe the evolution of propellant surface is analytically as seen in solid propellant rocket motor performance computer program (SPP). SPP is a popular SRM internal ballistics simulation software with three available analytic methods for grain design and evolution: two-dimensional, axisymmetric, and three-dimensional [5]. Because of complexity and lengthy computational requirements in setting up 3-D geometries, users are strongly encouraged to use the 2-D geometry over the 3-D method whenever possible.

The 2-D geometry design consists of defining several x–y planar cross sections (with lines and arcs), wherein the program assumes linear transference of port area and burning surface perimeter between cross sections [5]. The perimeter and port area for each cross section are calculated by scanning radially outward pointing rays for intersection with the grain. Surface evolution is conducted for linear segments using the normal of the line, and arcs by adjustment of the radius.

The axisymmetric grain design method is similar to 2-D, but instead uses a list of lines and arcs in the x–z or y–z plane assuming rotation around the rocket's central axis (z-axis). Geometry properties are calculated using closed-form analytical methods [5].

The 3-D geometry is quite involved, but may be necessary for certain rocket designs that prevent the use of the previous two methods in SPP. This uses a combination of nine analytical shapes to form the initial grain design: sphere, torus, plane, cylinder, cone, spheroid, hyperbolic torus, elliptical torus, and parabolic torus. The method of analysis consists of mapping the 3-D surface to a 2-D plane and checking several boundary conditions such as other burning surfaces, insulation, or user-specified dummy boundaries [5]. There may be up to 15 of these intersecting boundaries with each surface.

For purposes of reducing computation time, the grain design and internal ballistics module can be uncoupled from the ballistics module, which is a one-dimensional unsteady model. Also, SPP allows a combination of fully coupled and uncoupled surface advancement with the ballistics module for highly nonuniform grain regression.

Another way to model grain geometry is the phase-based analytical (numerical layering technique) method. When appropriate and possible, grid-based geometry methods can be replaced by analytical methods such as this to reduce computational time requirements. Analytical methods have been developed for several simple and complex cross-sectional geometries using numerical layering techniques [6,7]. This method breaks up the surface evolution process into several different phases within which the burning perimeter and port area at each cross section can be described mathematically. These phases describe time periods within which surfaces can be described by a single set of equations. Port area and burn perimeter are multiplied by grain length to acquire chamber volume and burning surface area, respectively.

The work described in this paper is part of an effort to develop a capability (called Rocballist) to simulate large-scale SRM behavior over time scales of the order of hundreds of seconds by using reduced physics equations. The goal is to retain enough complexity to maintain an accurate representation of grain geometry such that pressure and thrust accuracy is preserved. Because accurate representation of 3-D grain geometry evolution is a key requirement, the first part of this work is to develop a grain geometry capability, called Rocgrain. The fact that the burning rate variations in the radial and azimuthal direction are insignificant under many conditions motivates the development of a relatively simple tool that takes advantage of geometric simplifications associated with nearly constant burning rate at a given axial location but allows for axial burning rate variations. (Under certain conditions azimuthal and radial variations in burning rate can also occur, such as normal and lateral acceleration in spinning star-grain motors [8], radial propellant/casing vibration, or erosive burning. This situation is not addressed by the present model.) The goal of this work is to develop a fast, simple, three-dimensional, grain-geometry model that can handle initial complex SRM designs, burning surface regression, and surface evaluation for use in one-dimensional ballistics models with reduced physics. For the case of burning rate with azimuthal variations, the method developed in this paper is not applicable; instead, the level set method or face-offsetting method may be used.

The method used in this paper for generating an initial grain geometry representation and simulating evolution of the grain geometry corresponding to burnback of the propellant is the minimum distance function (MDF) approach. With reasonable assumptions about the solid propellant burning rate and orientation, the minimum distance to the initial surface can be used to represent the detailed shape (i.e., location) of the burning surface of the 3-D grain as it evolves in time. By manipulating the signed MDF to describe the motion of the solid propellant interface, in contrast to the level set method, there is no hyperbolic PDE to be solved. A companion paper [9] describes the development of a full motor simulation capability (Rocballist) by coupling this geometry tool (Rocgrain) with reduced internal flowfield equations to investigate the internal ballistics of SRMs.

II. Grain Geometry Initialization (MDF Calculation)

A. Introduction

Though axisymmetric, two-dimensional, and three-dimensional analytical geometries are often adequate for grain design and surface evolution models, they all require assumptions that may limit their application for internal ballistics simulations (i.e., for flowfield physics). Therefore, adequate representation of the burning surface of complex (nonanalytical) motor geometries requires a fully three-dimensional, numerical (i.e., computer-aided-design) geometry model.

One common method of representing three-dimensional surfaces is a signed minimum distance function. The MDF is based on a 3-D minimum distance grid (MDG) that is laid out over the volume of space occupied by the solid propellant and the gas core within it. The MDF is a scalar function whose magnitude at each grid point represents the distance from the grid point to the nearest point on the burning surface. The sign of the MDF indicates which side of the burning surface the grid point is on, i.e., whether the grid point is on the solid- or the gas-side of the interface. Thus, the burning surface is located between negative and positive MDF values where the MDF takes on the value of zero. For complex geometries, the analytic MDF calculation is not trivial, and hand calculation requires valuable time, which essentially eliminates grain design iterations and limits simulations to simple motors.

Computer-aided-design (CAD) programs are commercially available and offer user-friendly and thorough three-dimensional drafting capabilities. Nearly all offer an export option that converts the geometry to a stereo-lithography (STL) file format. A method has been developed to calculate the signed MDF using the surface stored in the STL file. This enables the use of CAD programs for the design of the initial grain geometry.

Because grain complexity can vary significantly even within the same motor, reduction in spatial grid resolution is attractive whenever possible. This is realized through the use of multiple minimum distance functions, each describing a different volume (or propellant segment) of the rocket with variable resolution. The procedure for the calculation of each MDF is the same.

B. Theory

1. STL File

A stereo-lithography file, typically used for rapid prototyping, is a three-dimensional surface representation used by CAD programs to approximate the surface of a solid using planar triangles. These triangles are listed in a data file by means of three vertices (listed counterclockwise when viewed in the negative facet normal direction) and their respective unit normal vectors. The CAD program will orient the normal vector to point outward of the drafted solid.

The number of triangles will vary depending on the propellant grain's complexity, curvature, and desired accuracy. The error introduced by the planar approximation can be controlled by the CAD export properties, but may be limited by the complexity of the design and required computing time. Higher accuracy will require more triangles for a better approximation of the surface, but will increase the MDF computation time.

For proper use of the MDF calculation method discussed next, the grain design must be drafted in the CAD program such that the rocket grain is concentric with the z-axis of the coordinate system used to output the STL file. It is also important that the chamber volume

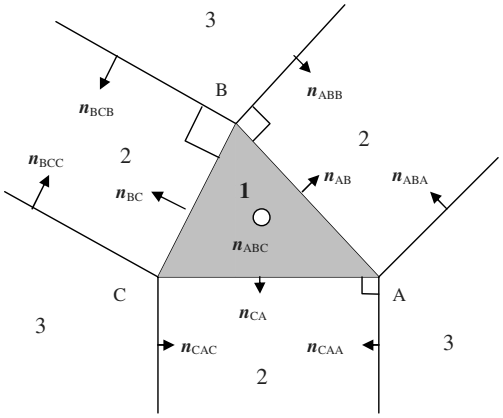

Fig. 1 Three divisions of space defined by a triangle.

(enclosed by the burning surface) must be drafted, not the solid propellant.

2. Program Overview

The task of calculating the MDF requires an individual calculation for each grid point to determine the shortest distance to each triangle representing the burning surface. To reduce computation time and ensure that the MDF is only calculated to burning surfaces, any triangles that fall outside the volume bounds of the MDG as well as triangles that do not represent a burning surface within this volume are eliminated.

There are three distinct volumetric regions defined by extruding a triangle normal to itself in space as shown in Fig. 1: the triangular cylinder extruded by the triangle (1), three semi-infinite slabs adjacent to the triangle sides (2), and three spaces between the slabs, adjacent to the triangle's vertices (3). The MDF calculation procedure varies depending on which region the grid point falls in: 1, 2, or 3. As shown in Fig. 1, a grid point will be closest to the plane of the triangle if it falls in region 1, to a line forming the edge of the triangle if it falls in region 2, and to a vertex of the triangle if it falls in region 3. These regions are defined by nine planes (or normal vectors) for each triangle and are initially calculated for future use in determining which MDF calculation method to apply.

Distance calculations between a point and a point (i.e., for a grid point in region 3 to a vertex) and between a point and a line (i.e., for a grid point in region 2 to the triangle edge) always have a positive sign associated with them. Using nearby triangles to determine where the grid point lies with respect to the surface, the sign of the MDF value is assigned by several methods described in detail in later sections of this paper.

3. Disadvantages

The main disadvantage of this method of calculating the MDF from a list of triangles is computation time. This method can become lengthy for a large grids because the order of the algorithm used is

$$\left(N_{\text{triangles}} \quad N_x \quad N_y \quad N_z\right)$$

Computation time will increase with both the grid size and the number of triangles listed in the STL file. Also, the MDF values will only be as accurate as the triangular surface approximation used in the STL file.

4. Advantages

Though computationally intense, the geometry initialization only needs to be run once for each grain design. This method calculates the correct (to double precision accuracy) MDF in all space of the user-controllable STL triangular surface approximation. Because of the compatibility with commercial CAD programs, knowledge of a new user interface is not required. Grain design modifications can be made easily, and the new MDF will be calculated with little human labor required. Additionally, the geometries can be easily transferred to other rocket simulation programs through various CAD files.

C. Method

1. MDG Definition and STL File Input

Several parameters in an input data file specify the size, location, and resolution of each MDG. A tight rectangular grid is formed over the rocket casing for each MDF calculation. The STL file, in ASCII format, is read in and corrected for rounding error by setting any values smaller than a given tolerance to zero. Rounding error arises from assignment of essentially random variables to values beyond the double precision accuracy (15 digits).

2. Triangle Elimination

Triangles are eliminated for two reasons. First, computation time can be reduced if triangles that lie beyond the range of that particular MDG are eliminated. This is accomplished by removing any triangles without a vertex located between the specified z-bounds of each particular MDG. Second, the MDF must be calculated only to the burning surface, so any triangles that represent an inhibited or nonburning surface must be removed. The x–y oriented end planes are removed by checking if all three triangle-vertices lie at a user-specified eliminated z-location. The result is faster MDF calculation because the number of triangles is reduced to only the burning surfaces located in the MDG.

Though multiple MDGs can significantly reduce computation time, they must be used correctly to avoid error. Because the MDF will be calculated only to the triangles located within the bounds of the MDG, the temporal burning surface (the isodistance contours) will only represent the MDF for the surface represented by those triangles. Any burning surface that propagates from one MDG into another will be incorrectly modeled. Therefore, the MDG definition must ensure that no burning surface will burn into another MDG's spatial domain throughout the full rocket burn. The opposite holds as well: no burning surface should be allowed to propagate outside the volume defined by the MDG. Also, for sign correction purposes, any eliminated x–y planes must lie on the upper or lower z-bounds of the MDG.

3. Triangle Normal Vectors Definition

There are several important normal vectors necessary to define the different regions of space of each triangle (see Fig. 1). As these normal vectors are used many times, redundant calculations are reduced by initially calculating and storing all normal vector information for each triangle. The nine normal vectors shown in Fig. 1 are calculated for all noneliminated triangles. Note: $\boldsymbol{n}_{\text{ABC}}$ is known from STL file. The six vectors on the extended lines are calculated by subtracting one vertex from the other. The calculation for the three outward pointing normal vectors is done by crossing three of the six aforementioned vectors with $\boldsymbol{n}_{\text{ABC}}$. For example, $\boldsymbol{n}_{\text{AB}}$ is calculated by crossing $\boldsymbol{n}_{\text{ABA}}$ into $\boldsymbol{n}_{\text{ABC}}$.

4. Grid Point to Plane Distance Calculation

For each grid point, the plane distance calculation calculates the distance to all noneliminated triangles if and only if that point lies in the respective planar region (i.e., within $-\boldsymbol{n}_{\text{AB}}$, $-\boldsymbol{n}_{\text{BC}}$, and $-\boldsymbol{n}_{\text{CA}}$ as defined in Fig. 1). The distance from a point to a plane is determined by the dot product of the plane's unit normal vector and a vector pointing from any point on the plane to the point of interest:

$$d = n_x(x_{i,j,k} - a_x) + n_y(y_{i,j,k} - a_y) + n_z(z_{i,j,k} - a_z) \qquad (1)$$

where (n_x, n_y, n_z) are the components of unit normal vector of a plane $\boldsymbol{n}$, $(x_{i,j,k}, y_{i,j,k}, z_{i,j,k})$ are the coordinates of grid point at (i, j, k), and (a_x, a_y, a_z) are the coordinates of any vertex of the triangle considered.

The sign will be correct as the normal vector is defined to point outwards (towards the solid propellant), and therefore positive

values will lie in the solid propellant, and negative in the chamber volume.

5. Grid Point to Line Distance Calculation

The signs of the distance to the nine planes in Fig. 1 are used to determine in which (if any) of the three linear (planar slab) regions (2 in Fig. 1) the grid point lies. If it falls in one of the linear regions, the distance from the grid point to the line of interest is calculated using standard dot product methods.

Because the calculation for the distance to a line in space will yield a positive value, the sign may or may not be correct and a sign assignment is necessary. This is only done once per grid point if the calculated distance is smaller than what is currently stored. If these requirements are met, the adjacent triangle that shares the line of interest is determined. Depending on the local orientation and status of the two triangles of interest, three methods are employed to find the sign of the minimum distance value: two fast and one more lengthy.

Method 1 is used if the adjacent triangle is an eliminated triangle. The sign of the MDF value is determined by evaluating the distance from the grid point to the noneliminated triangle's plane. This method of determining the proper sign requires any eliminated triangles to be located at the upper or lower z-bounds of the MDG. Therefore, if x–y surfaces require inhibition within the rocket grain, multiple MDGs must be used such that they begin/end at that location.

Method 2 is used when the triangles that make up that line are at a large angle to each other (see Fig. 2). When the dot product of the two triangles' normal vectors is greater than or equal to zero, the angle (θ) is greater than or equal to 90 deg and therefore "large." In this case, the sign of the distance from the grid point to either triangle's plane is assigned to the MDF value.

Occasionally, the grid point lies directly on one of the planar extensions (the lightly dotted lines in Fig. 2). In this case the distance is evaluated to the other triangle's plane, and its sign is recorded. In an even more rare case, the grid point lies exactly on both planes, which only happens when the grid point lies exactly on the line of interest, and thus the surface. In this case, the minimum distance is essentially zero and no sign correction is necessary.

Method 3 is required once the inside angle between the two triangles becomes smaller than 90 deg (Fig. 3). The sign of the distance from the grid point to the triangles' planes will be different depending on which of the three regions the grid point lies in, so a more involved method is required.

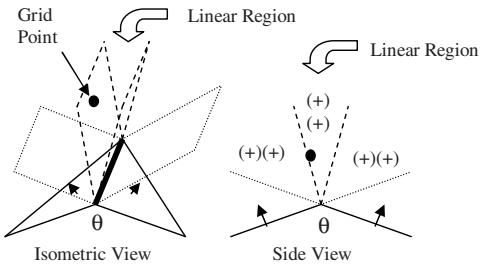

Fig. 2 Method 2: large angled line sign correction.

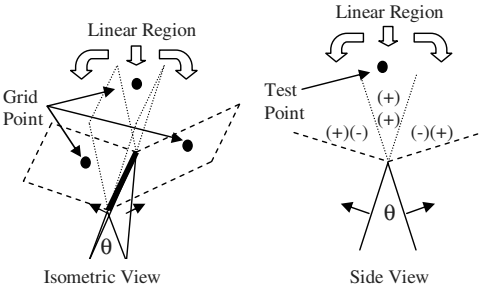

Fig. 3 Method 3: small angled line sign correction.

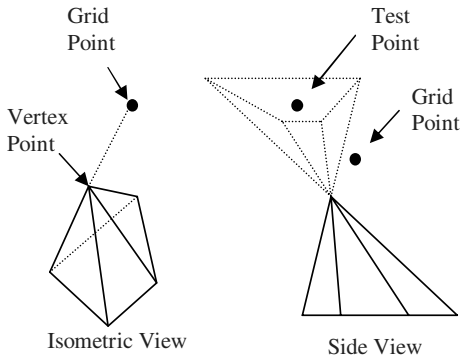

Fig. 4 Point to vertex sign correction.

The sign assignment method for this case uses a test point, which is created such that it will always fall within the middle region of the side view of Fig. 3. Two vectors (one for each triangle) are created that point from the triangle's vertex not on the line to the middle of the line of interest. The test point is defined by adding those vectors to the point bisecting the important line. The sign of the distance from the test point to either triangle's plane will be the same, and is assigned to the MDF value.

6. Grid Point to Vertex Distance Calculation

The distance from each grid point is calculated to each nonredundant vertex. If the magnitude of the distance is smaller than the current MDF value, sign correction is necessary. This requires finding all noneliminated triangles that share the vertex of interest (the point that the grid point is closest to). A vector is created by summing a set of vectors from the center of each triangle to the vertex point. The test point is acquired by adding this vector to the vertex point itself (see Fig. 4). The sign of the distance from the test point to the set of triangles' planes is assigned as the MDF value.

D. Limitations and Restrictions

The MDG location and resolution must be defined using the same coordinate system used in the CAD program. Any triangles representing nonburning surfaces *must* be eliminated or the minimum distance will be calculated to them. Only x–y planes located on the upper and lower z-bounds of the MDG may be eliminated.

Nonconvex hull-type, sharp-angled cones that point inwards (towards the chamber volume) may cause a sign error. The magnitude of the distance will be correct, but the sign may be positive when it is supposed to be negative. However, no practical rocket grain designs exist with such a design.

E. Results

To test and illustrate the capabilities of this approach, several hypothetical and real SRM grains have been examined. The grains have been drafted in Pro-E and exported in STL format. The MDF was calculated using the approach described in preceding sections (Rocgrain) and plotted using Matlab. Figure 5 contains a Pro-E screen capture of a hypothetical SRM composed of a 10-finned star pattern and a circular cylinder.

Two-dimensional distance contour plots of the MDF crossing the cylinder and star pattern sections are shown in Figs. 6 and 7 respectively. Notice that each distance contour could be acquired by advancing the zero-level surface a certain distance normal to itself.

When the MDF is calculated to every triangle (i.e., no removed surfaces) the 3-D zero-level surface shown in Fig. 8 is acquired. However, in many SRM designs some end surfaces are nonburning (inhibited or insulated), and therefore it is desirable to remove them as shown in Fig. 9.

The MDF has also been calculated for more complicated motor designs, such as the Naval Air Warfare Center (NAWC) tactical motor series used for nonlinear acoustic instability testing [10]. Motor No. 6 in the second series [10] has been drafted to scale in Pro-

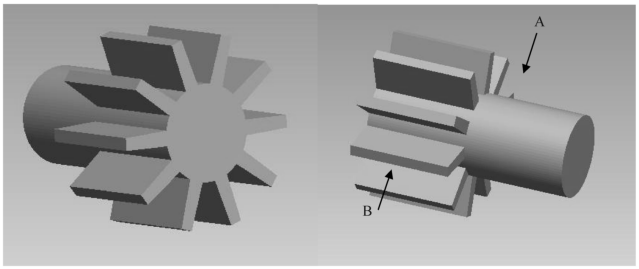

Fig. 5 Pro-E screen capture: hypothetical SRM.

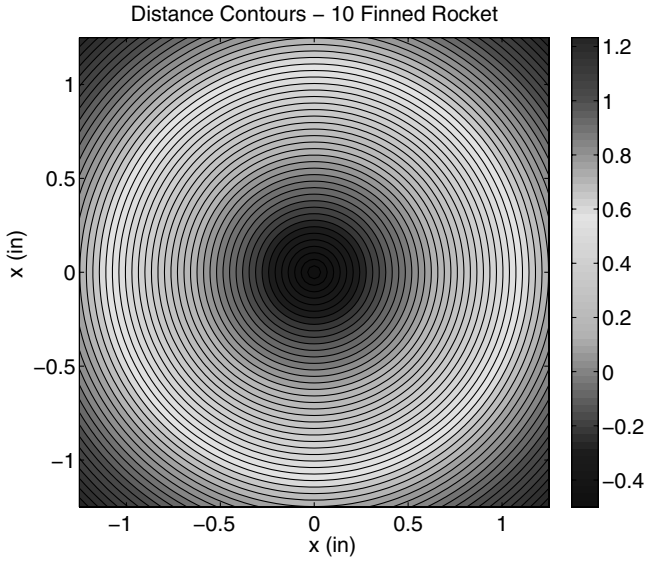

Fig. 6 2-D distance contours for Fig. 5 (A).

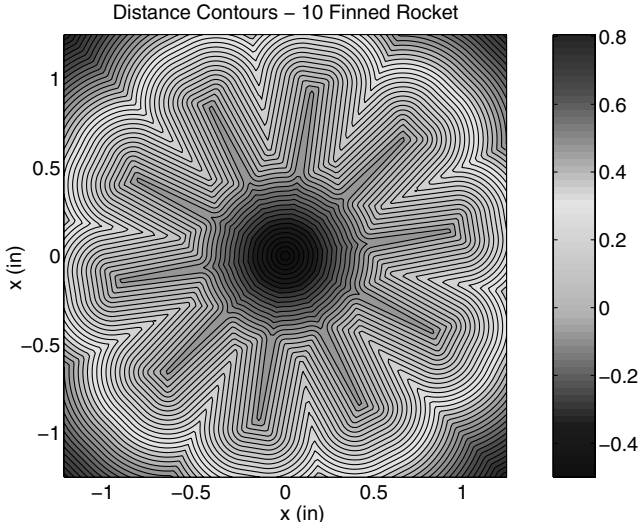

Fig. 7 2-D distance contours for Fig. 5 (B).

E (Fig. 10) using initial grain geometry specifications reported in [11]. This motor is a star-aft configuration [10], with the nozzle (not shown) located on the right in Fig. 10.

The MDF for NAWC Motor No. 6 has been calculated by Rocgrain. As there are four different types of cross sections in the grain and over 7000 triangles in the STL representation, four MDGs with variable spatial resolution have been used for the analysis. These results show that Rocgrain is quite capable of treating realistic, 3-D solid rocket grains. Furthermore, the initial CAD creation of the geometry is relatively straightforward based on standard CAD software and commands.

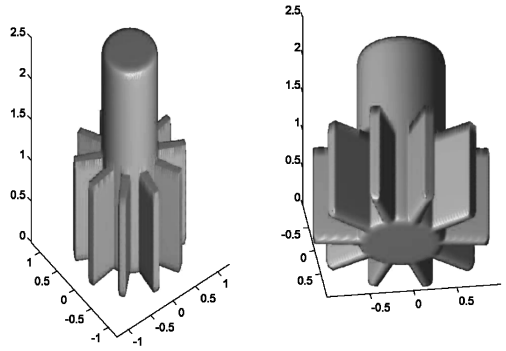

Fig. 8 Zero-level surface (with ends).

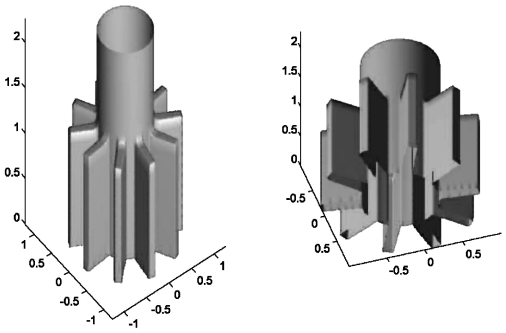

Fig. 9 Zero-level surface (without ends).

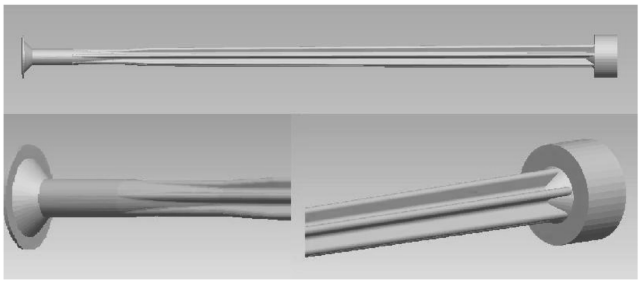

Fig. 10 Pro-E screen capture: NAWC Motor No. 6.

III. Surface Evolution

A. Introduction

The capability to determine the signed minimum distance function for complex geometries within the domain of interest can be used for more than just locating the initial surface. Using reasonable assumptions, the MDF of the initial surface can be used to represent the three-dimensional shape and location of the solid propellant's burning surface as it evolves in time. Rocgrain takes advantage of the fact that the radial and azimuthal variations in burning rate are often negligible to model the evolution of propellant surface during the burn. The value of burning rate at an axial location is used in the radial and azimuthal directions corresponding to that axial location to manipulate the MDF. By assuming the burning rates are uniform in radial and azimuthal directions, the computer time is significantly reduced compared to other three-dimensional surface evolution models. And the effect of the burning rate variations in axial direction is preserved: consistent with the first-order significance in the axial direction of an SRM. Coupled with the axial burning rate variations obtained from flowfield calculation, the propellant surface evolution can be accurately simulated. Rocgrain, in turn, calculates the burning perimeter, wetted perimeter, and port area along the rocket axis in one-dimensional simulations to provide necessary information to flowfield solver.

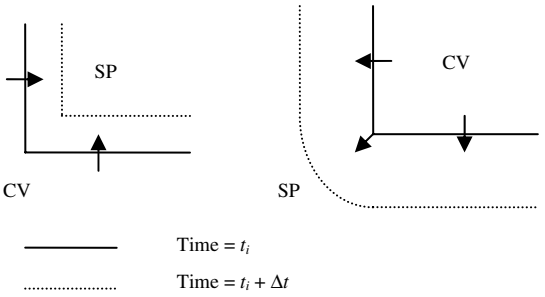

Fig. 11 Sharp corner evolution.

B. Theory

As discussed, the burning surface of the solid propellant is determined by the zero-level contour of the minimum distance function. However, the nonzero isodistance contours to the initial surface can be used to represent the temporally dependent three-dimensional burning surface. This is possible assuming that the burning rate is constant both temporally for a given time step and spatially over a given x–y cross section, and that the burning surface will propagate normal to itself in three dimensions. The new surface is represented by the zero-level contour of a new MDF calculated by subtracting a scalar "burnt distance" (representing the product of a time step and burning rate) from the initial MDF:

$$d_b = \Delta t^* r_b \tag{2}$$

Because of its simplicity, this method significantly reduces computation time when compared to most three-dimensional surface evolution methods. Surface meshing and remeshing are eliminated. There is no need to calculate the local surface orientation, as the surface will propagate normal to itself. Also, where the derivative of the surface is discontinuous (corners or sharp edges), the future surface is represented correctly without further corrections. When a sharp corner is external-burning (left side of Fig. 11) the sharp corner is preserved; when it is internal-burning (right side of Fig. 11) the corner smoothes to a semicircular arc. This evolution is handled naturally by the MDF.

C. Method

1. *Surface Evolution*

Surface evolution is completed independently for each two-dimensional (x–y) set of MDG points. The burnt distance for each z-location is calculated independently by the temporally dependent (axially variable) local burning rate and time step. If the burning rate is constant along the z-axis, such as for 0-D models, then the burnt distance is calculated by the product of a spatially constant but temporally dependent burning rate. The ability to handle axial variations of burning rate (e.g., erosive burning and axial pressure drop effects) is crucial for many SRM designs and allows this surface evolution method to better represent what physically occurs.

2. *Propellant Burnout*

Because the MDF represents only the burning surface in a rectangular grid, the only knowledge Rocgrain has of the propellant/insulation or propellant/case interface is from a user-defined radius. A correction is necessary to prohibit any burning surface area contribution from portions of the burning surface that have reached this "burnout interface." This correction is also required for proper wetted perimeter and port area evaluation. The wetted perimeter is the length that bounds the port area (burning plus nonburning surface).

All MDF values outside the burnout interface should always be positive, so that no burning surface area is allowed beyond the insulation/case. This is accomplished by overwriting any negative MDF values outside the burnout interface to a small (but positive) number at each time step. This method has been used for two reasons. First, any interpolation near the surface between the small positive number and a negative MDF value (inside the burnout interface) will force the intersection point (intersection of burning surface with MDG lines) to lie *outside* the interface. When any burning surface intersects the MDG outside the burnout interface, the intersection point is adjusted either horizontally (along x) or vertically (along y), depending on which type of grid line it crosses such that it falls directly on the interface. If this correction occurs, a flag is triggered that prevents any local burning surface area contribution. The corrected intersection point is used for the port area and wetted perimeter calculation, but burning perimeter from that local section is set to zero. Second, seeing as values are not reset until they become negative, any burning surface (before crossing the burnout interface) will have the proper MDF values to accurately locate the surface via interpolation. If this surface lies outside the burnout interface, the same correction is applied to eliminate local contributions to the burning perimeter. This provides a three-dimensional analysis for certain portions of the solid propellant contacting the insulation/casing before others.

D. Surface Evolution Error Assessment

The two basic assumptions in the surface evolution model are that the surface burns normal to itself and at a constant rate for the duration of the surface advancement time step. For zero-dimensional internal ballistics simulations, no further assumptions or approximations are required. The new MDF will represent the surface exactly as if it had burned normal to itself for the specified distance.

However, coupling of Rocgrain with one-dimensional internal ballistics simulations (allowing z-axis variations in surface propagation rate) requires further assumptions. Because the burning rate will most likely vary with axial location, the surface will propagate normal to itself at different speeds depending on the surface's local burning rate. Therefore the burnt distance should be calculated by the burning rate at the surface that the grid point represents, not the burning rate at the grid point's spatial location. If the motor geometry is such that any surface normal has a component in the z-direction, these burning rates may be different.

For example, in a conical grain design such as Fig. 12, the MDG point that contains the distance to (x_s, y_s, z_s) on the burning surface will not be located in the same x–y plane as z_s unless the distance is zero (i.e., the MDG point lies on the surface). Therefore, when advancing the surface, the MDF at $(x_{i,j,k}, y_{i,j,k}, z_{i,j,k})$ gets subtracted an effective burnt distance based on the burning rate at $z_{i,j,k}$, not z_s. There will be no error introduced when the surface is not changing in the z-direction (e.g., straight cylinder, star pattern, etc.).

Three things must happen simultaneously for this situation to introduce significant error. First, the burning rate must change significantly in this distance $(z_{i,j,k} - z_s)$, the angle of the "cone" must be large, and the $(x_{i,j,k}, y_{i,j,k}, z_{i,j,k})$ point must be far away from the surface so that error can accumulate. This has not been the case with the rocket motors analyzed.

E. Results

As the results for surface evolution are three-dimensional surfaces in time, the best way to view them is by movies; nevertheless, for the purpose of this paper several pictures have been included that show

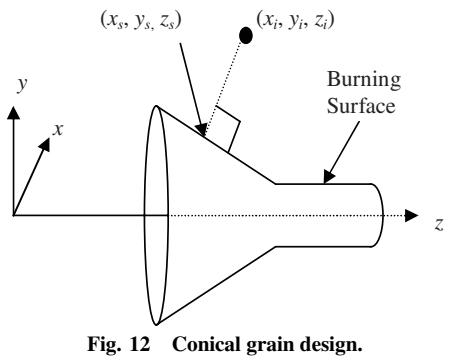

Fig. 12 Conical grain design.

the time evolution (at a constant burning rate of 1.0 cm/s) of the burning surface of NAWC tactical motor no. 6 (Fig. 13). This motor was selected because of its geometric and ballistic complexity. It is a full-length star-aft grain design that has end-burning sections, variable cross section star patterns, inhibited surfaces, and burning surface contacting the insulation/case at various times. Full-length means that the length of the motor is about 2 m, as opposed to some 1-m half-length motors that were also used in the China Lake program [10].

Notice that not all the solid propellant reaches the rocket insulation/case at the same time. Though burnt surface area shows up in the plot as a cylinder, any portion beyond the rocket casing has been corrected not to contribute to the burning surface area in the Rocgrain model.

IV. Chamber Volume and Surface Area Calculation

A. Introduction

We have shown how the three-dimensional surface can be evolved using the initial grain geometry and the minimum distance function as a basis. However, to use this surface evolution theory, the burning surface must be both located and quantified. For use in ballistics models, grain geometry properties such as burning surface area and chamber volume are required (1-D models require burning perimeter and port area at each cross section). This must be done in a way that accounts for end-burning sections and certain portions of the burning surface reaching the insulation/case before others.

B. Theory

The use of a one-dimensional ballistics model was anticipated, so each x–y plane of the MDF is analyzed to acquire geometry profiles as a function of axial location. Any two neighboring MDF values with opposite signs (i.e., negative product) will have a burning surface between them. Intersection points between the burning surface and the minimum distance grid lines are calculated using linear interpolation. Knowledge of the intersection points allows the local burning (and wetted) perimeter and port area to be calculated.

C. Method

1. Program Overview

The one-dimensional geometry arrays (burning perimeter, wetted perimeter, and port area) area acquired from the analysis of each x–y plane of each MDF. After the 1-D burning perimeter and port area have been calculated, total rocket properties (burning surface area and chamber volume) are acquired by numerical integration of the axial geometry profiles. The MDF is also evaluated for end-burning surfaces; any end-burning surface area contributions are added to the total burning surface area. Each MDF is also checked for burnout for reduction in computation time in the next time step.

Because the volume bounded by the MDG(s) (i.e., the solid propellant grain) may not span the entire length of the rocket, any additional volume contained by the casing and nozzle must be added to the chamber volume. The rocket specification data in the geometry input file are used to calculate the additional chamber volume not enclosed by the MDG(s) from the head end to the throat. The nozzle volume is calculated by numerical integration assuming a circular cross section.

2. 1-D Geometry Analysis

For each 2-D slice of the MDG, the x–y grid points are iterated through and the perimeters and areas summed. The surrounding MDF values are used in a two-dimensional analysis to determine if, where, and how much burning perimeter and port area is located within a given square (see Fig. 14). The perimeter is determined by the length of the burning surface that intersects the grid square. Section III elucidates how this is accomplished.

Once the entire MDG is iterated through, an extrapolation correction is conducted in the first time step for purposes of eliminating errors due to end-burning section grid noise. The first and last ($z_{\min}$ and $z_{\max}$) grid points' perimeters (burn and wetted) are predicted from a second-order extrapolation as shown in Eqs. (3) and (4). If the current value is not within a specified tolerance of the predicted value, the predicted value is used for the 1-D geometry information.

$$P_{0\text{predicted}} = P_1 - \Delta z \frac{(-3P_1 + 4P_2 - P_3)}{2\Delta z} \tag{3}$$

$$P_{nz\text{predicted}} = P_{nz-1} + \Delta z \frac{(3P_{nz-1} - 4P_{nz-2} + P_{nz-3})}{2\Delta z} \tag{4}$$

3. Find Surface

The workhorse of Rocgrain is a module that locates the surface and calculates various geometric properties of each grid point. Non-end-burning surfaces are evaluated using a two-dimensional analysis for a grid square as shown in Fig. 15. End-burning section analysis is conducted by evaluating the MDF in the z-direction (Fig. 16). Each method is discussed in detail in the following subsections.

a. Non-End-Burning Sections. The burning surface is located by interpolation between opposite signed MDF values. The method of quantifying the perimeters and areas varies depending on how many corners (total of four) are positive, negative, or zero. If all are positive or negative, the square lies completely in the solid propellant or gas (combustion chamber), respectively. Otherwise a burning perimeter, wetted perimeter, port area, and solid propellant area must be calculated, which requires the burning surface to be located.

To locate the surface, each pair of MDF values whose product is nonpositive is linearly interpolated using their respective locations. As the zero contour defines the surface, each point that intersects the square of interest can be calculated. An example of the method used to locate the intersection points (P_1 and P_2 in Fig. 16) is shown in Eqs. (5) and (6):

$$P_1 = \left\{ \left[x_{i,j,k} + \Delta x^* \left(\frac{|\text{MDF}_{(i,j+1,k)}|}{|\text{MDF}_{(i,j+1,k)}| + |\text{MDF}_{(i+1,j+1,k)}|} \right) \right], \; y_{i,j,k} + \Delta y, z_{i,j,k} \right\} \tag{5}$$

$$P_2 = \left\{ \left[x_{i,j,k} + \Delta x^* \left(\frac{|\text{MDF}_{(i,j,k)}|}{|\text{MDF}_{(i,j,k)}| + |\text{MDF}_{(i+1,j,k)}|} \right) \right], y_{i,j,k}, z_{i,j,k} \right\} \tag{6}$$

The distance between these intersection points is calculated for the perimeter contribution. If neither point lies outside the burnout interface, then that length is added to the burning and wetted perimeter for that z-location. Otherwise, it is only added to the wetted perimeter. Note that this method approximates any curved surface by a series of straight lines which will underpredict the true perimeter. Both the solid propellant area and port area are also calculated using these intersection points. These areas are summed to their respective one-dimensional data arrays.

The underlying assumption for Eqs. (5) and (6) is that the proportionality between the MDF values and the surface's location between the two points is approximately the same. This assumption breaks down near end-burning surfaces as the two MDF values may represent two different surfaces. Also, because the surface is approximated with straight lines, error may be introduced if the grid is not appropriately sized near surfaces with high local curvature. This method has not been found to introduce significant error with appropriate grid refinement.

b. End-Burning Section Evaluation. End-burning sections are evaluated for each grid point using neighboring MDF values along the z-axis. If the product is negative or zero, a check of the surrounding points is required to know whether this is a true end-burning section or just an occurrence of solid propellant crossing the

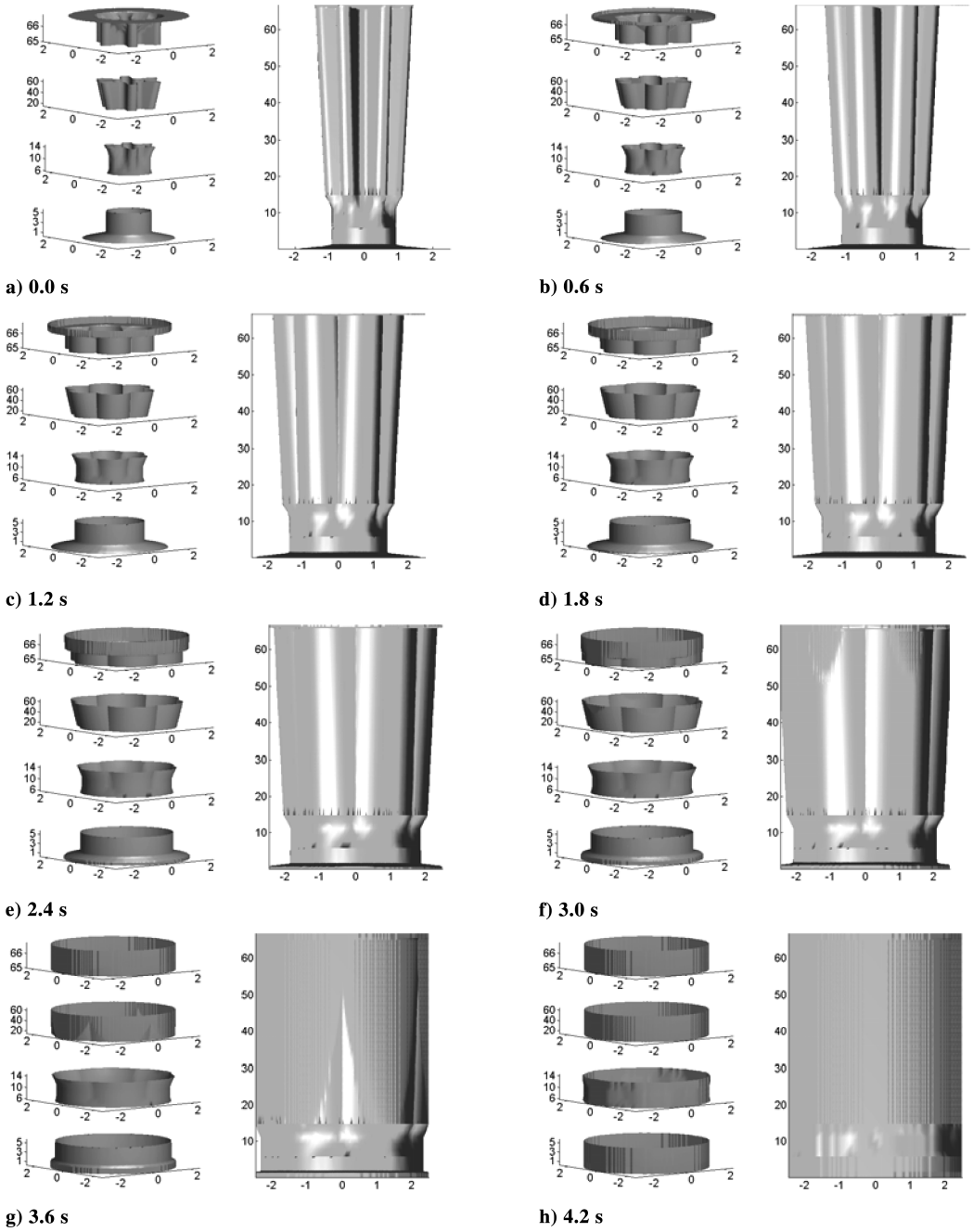

Fig. 13 Motor No. 6 propellant surface evolution.

z-plane. This involves comparing the distance of the grid point to the surrounding points (see Fig. 16).

Because end-burning sections are oriented in the x–y plane, the distance to the surface for several of the surrounding points in each x–y plane will equal each other. Not all MDF values will necessarily equal each other if the grid points are close to the rocket case or other burning surfaces. However, if at least eight points have similar distances, the surface is determined to be an end-burning surface and its surface area ($\Delta x^* \Delta y$), orientation (left or right), and z-location (from interpolation) are stored.

D. Results

1. *Rocgrain Verification*

For increasing grid sizes (i.e., reduced grid spacing), Rocgrain geometry properties should converge to what is calculated analytically by Pro-E. Two hypothetical grain designs have been analyzed for this type of verification: object A is a simple cylinder and object B is a 12-point star pattern (see Fig. 5). The resolutions of STL (triangular) surface approximation are:

Geometry A: Max error due to Pro-E STL file approx.= 0.000254 cm, 628 triangles

Geometry B: Max error due to Pro-E STL file approx.= 0.000508 cm, 332 triangles

As can be seen in Figs. 17 and 18, both objects converge towards the analytical surface area and chamber volume with increasing grid size when evaluated by Rocgrain. Note that as the number of grid points approaches infinity, the geometry properties will converge to the triangular surface approximated surface area (SA) and chamber volume (CV), which are always slightly less than the true analytical values.

The percent error in numerically vs analytically calculated surface area and chamber volume has also been calculated and shown in Figs. 19 and 20. Notice that for the same level of accuracy, a lower grid resolution is required for the cylinder than for the star pattern. Also the rate of convergence is higher for the cylinder. This is expected because multiple sharp edges in object B require better grid

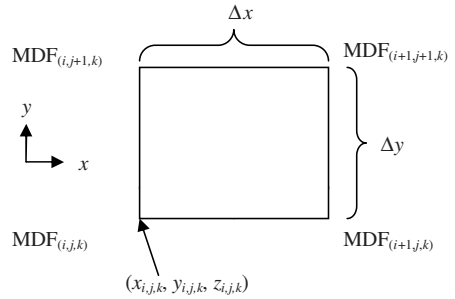

Fig. 14 Surface location grid square.

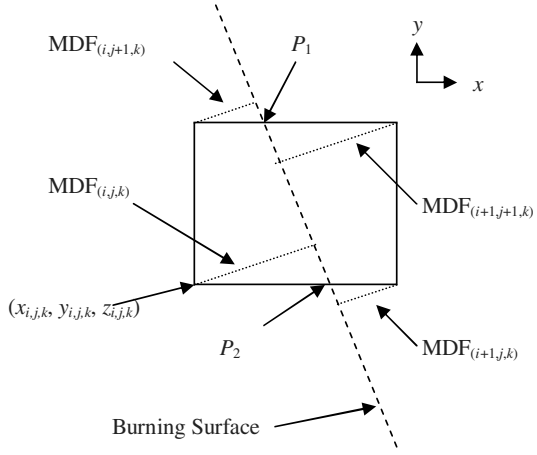

Fig. 15 Surface location example.

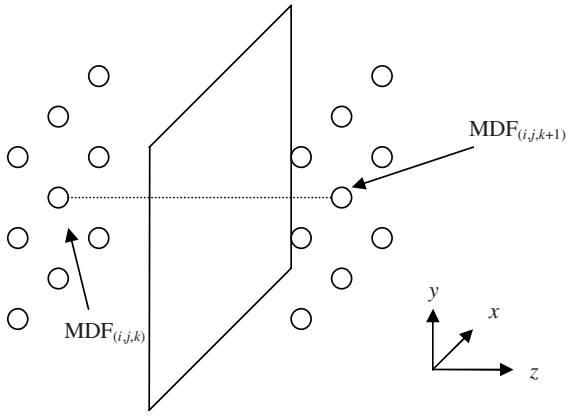

Fig. 16 End-burning surface evaluation.

resolution to accurately locate the surface. The percent error of chamber volume does not monotonically decrease as the number of grid points increases. Minimum percent error occurs at the case with 200 grid points, which might be because the discretized grid points align optimally with the physical grain geometry.

The surface evolution model has also been evaluated for these objects. The results for the cylinder match the analytical results in time to within 0.15% for a grid size of 21 × 21 (Fig. 21). However, there are no known analytic results for the temporal evolution of the 12-finned star pattern (Fig. 22). The maximum percent deviations of burning surface area from analytical result for other grid sizes are 0.035, 0.019, 0.014, 0.013, 0.011, 0.010, 0.0096, and 0.0090 for 51 × 51, 101 × 101, 151 × 151, 201 × 201, 301 × 301, 401 × 401, 501 × 501, and 601 × 601, respectively. Also, the analytical burnout time required for a 1.27 cm (0.5 in.) radius cylinder burning towards a 1.905 cm (0.75 in.) case at 1.0 cm/s (0.3937 in./s) is 0.635 s. The burnout time using the 21 × 21 grid size is predicted to occur at 0.63576 s, within 0.12% of analytical. For the 12-finned star grain, the maximum deviations of burning surface area (>40.0 cm^2)

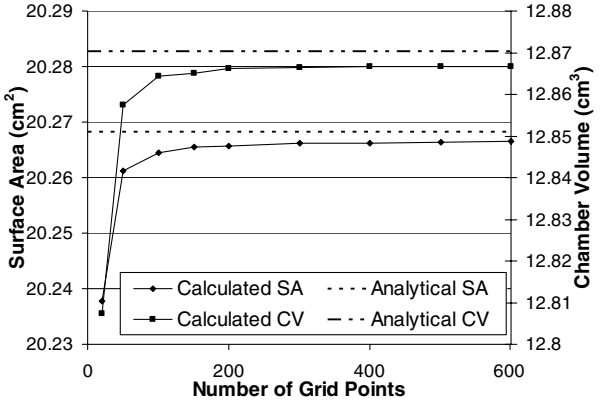

Fig. 17 Grid convergence (case A) of surface area and chamber volume.

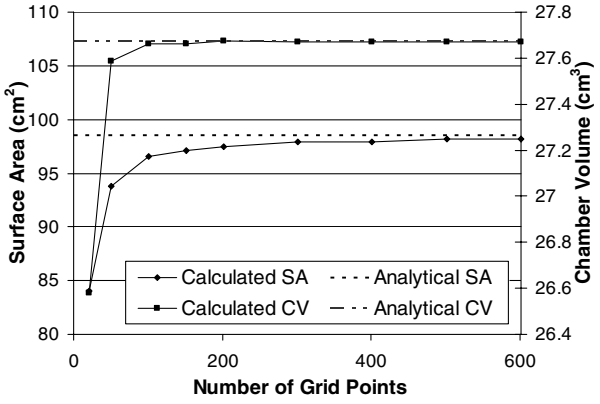

Fig. 18 Grid convergence (case B) of surface area and chamber volume.

between the finest grid (601 × 601) and coarser grid sizes are 25.0, 11.4, 6.29, 4.05, 2.86, 1.49, 1.10, and 1.00% for the 21 × 21, 51 × 51, 101 × 101, 151 × 151, 201 × 201, 301 × 301, 401 × 401, and 501 × 501 grids, respectively.

To summarize, geometries with sharp flat surfaces are faster to calculate the initial MDF due to the reduced number of triangles required for surface approximation. However, sharp angles require increased resolution for surface area and chamber volume calculation. The opposite is also true: curved surfaces require more triangles and hence a longer MDF calculation, but surface area and chamber volume calculations will not require as much grid refinement.

2. *NAWC Motor No. 6*

The grain evolution and temporally varying geometry properties have been calculated using Rocgrain for NAWC [9] Motor No. 6 with constant burning rate of 1.0 cm/s. The geometry properties (burning surface area, chamber volume, and solid propellant volume)

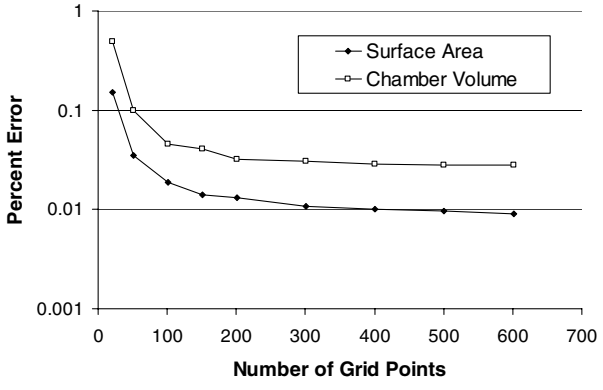

Fig. 19 Percent error of surface area and control volume (case A).

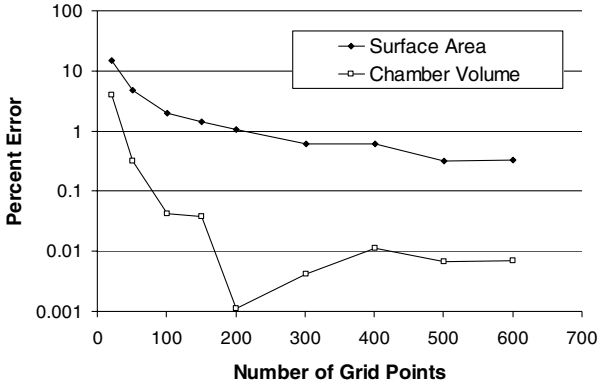

Fig. 20 Percent error of surface area and control volume (case B).

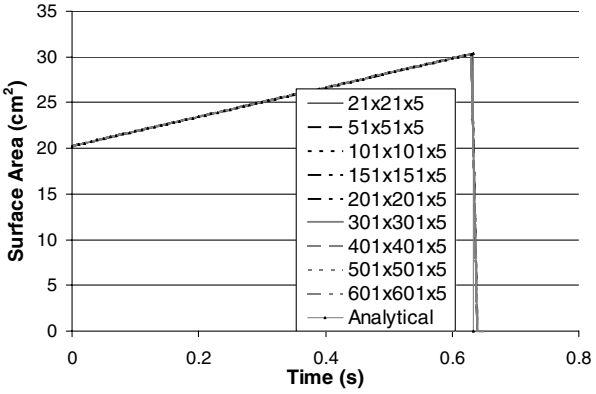

Fig. 21 Effect of grid size on history of surface area (case A).

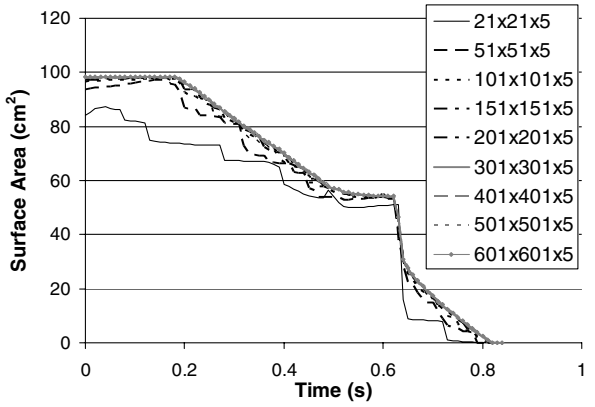

Fig. 22 Effect of grid size on history of surface area (case B).

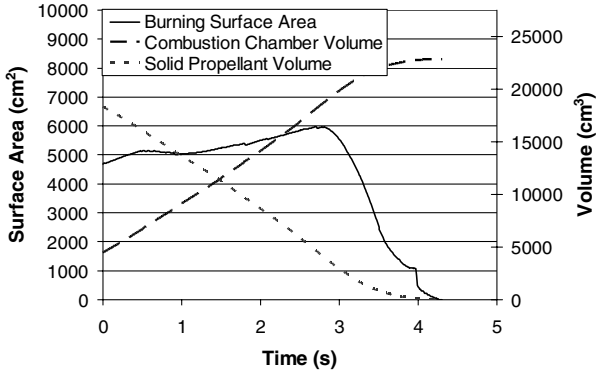

Fig. 23 NAWC Motor No. 6: total propellant geometry properties.

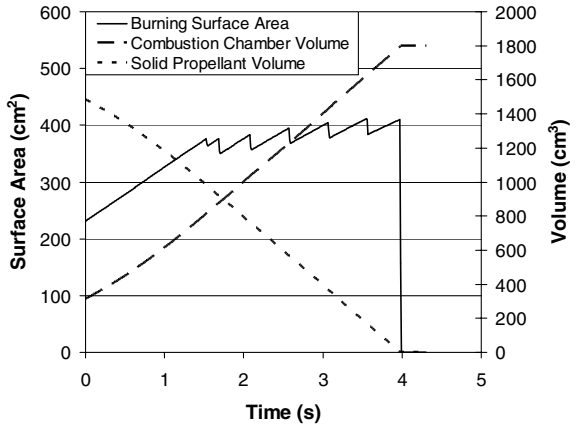

Fig. 24 NAWC Motor No. 6: propellant geometry properties of segment 1 (MDF 1).

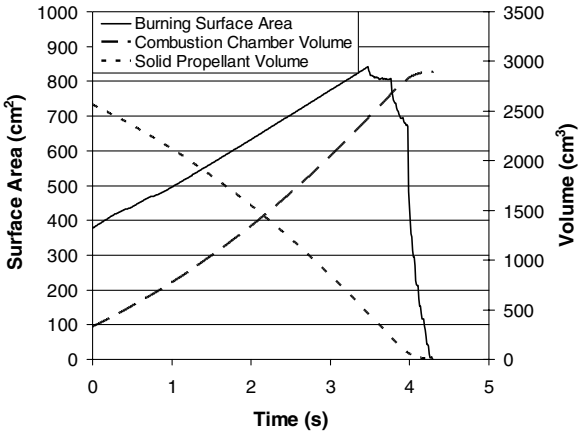

Fig. 25 NAWC Motor No. 6: propellant geometry properties of segment 2 (MDF 2).

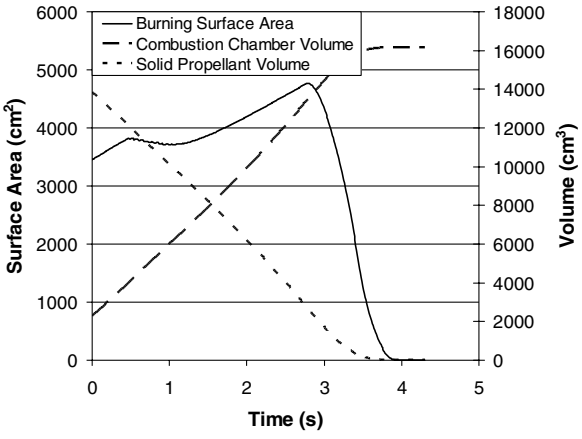

Fig. 26 NAWC Motor No. 6: propellant geometry properties of segment 3 (MDF 3).

for the entire rocket and each of four individual minimum distance functions have been plotted in Figs. 23–27 with the following ranges:

MDF 1: $z = 0.4826$–14.681 cm (0.19–5.78 in.)
MDF 2: $z = 14.681$–37.541 cm (5.78–14.78 in.)
MDF 3: $z = 37.541$–165.10 cm (14.78–65.00 in.)
MDF 4: $z = 165.10$–169.62 cm (65.00–66.78 in.)

Figure 23 shows the evolution of the burning surface area and total chamber volume for the entire motor and Figs. 24–27 show the same thing for the individual propellant segments. Results indicate that whereas the regression pattern of total burning surface area is relatively mild, the regression pattern of individual propellant segments can be strong and sometimes go in opposite direction (i.e., regressive vs progressive). Notice that as the surface in the various

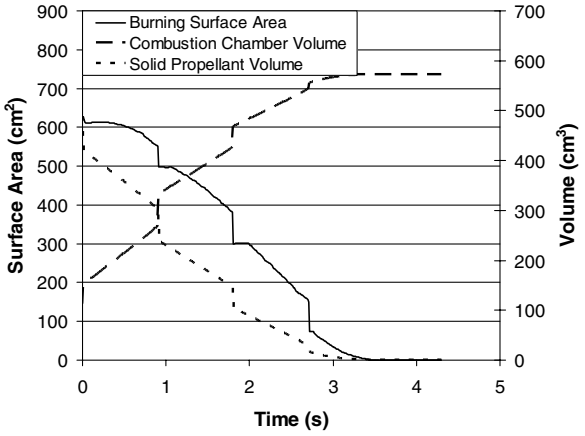

Fig. 27 NAWC Motor No. 6: propellant geometry properties of segment 4 (MDF 4).

fuel segments reaches the rocket casing, the burning surface area approaches zero. The noise seen in the surface area profiles is due to grid resolution. If necessary, this can be smoothed by further grid refinement.

V. Conclusions

The use of the signed minimum distance function for three-dimensional SRM grain initialization and evolution has several advantages. Compatibility with CAD programs allows well-developed drafting methods to be used for complex SRM grain design in both Rocgrain and other grain regression models. The capability to allow axially varying burning rate (due to pressure drop or erosive burning contributions) allows for a reasonably realistic surface evolution model and internal ballistics calculations. The capabilities of variable grid resolution, dynamic time stepping, elimination of meshing, solution of insulation/case burnout, and simple sharp edge/corner evolution make the MDF method attractive. The coupling of Rocgrain with a one-dimensional flowfield physics model (Rocballist) is discussed in a subsequent paper.

Acknowledgments

Suggestions for initial minimum distance function calculation methods by Sunhee Yoo and funding for this work from the University of Illinois Center for Simulation of Advanced Rockets research program, supported by the U.S. Department of Energy through the University of California under subcontract B523819, are gratefully acknowledged. Any opinions, findings, and conclusions or recommendations expressed in this publication are those of the authors and do not necessarily reflect the views of the U.S. Department of Energy, the National Nuclear Security Agency, or the University of California.

References

[1] Zeller, B., "Solid Propellant Grain Design," *Solid Rocket Propulsion Technology*, 1st ed., edited by A. Davenas, Pergamon, New York, 1993, pp. 35–84.

[2] Gossant, B., "Solid Propellant Combustion and Internal Ballistics," *Solid Rocket Propulsion Technology*, 1st ed., edited by A. Davenas, Pergamon, New York, 1993, pp. 111–192.

[3] Sethian J. A., *Level Set Methods and Fast Marching Methods*, Cambridge University Press, Cambridge, England, 1999.

[4] Yildirim, C., and Aksel, M. H., "Numerical Simulation of the Grain Burnback in Solid Propellant Rocket Motor," AIAA Paper 2005-4160, July 2005.

[5] Hermsen, R. W., Lamberty, J. T., Jr., and McCormick, R. E., "Volume V: User's Manual for the SPP Grain Design and Ballistics Modules," The Solid Propellant Rocket Motor Performance Computer Program (SPP), Version 6.0, Software and Engineering Associates, Carson City, NV, Dec. 1987.

[6] Hartfield, R., Jenkins, P., Burkhalter, J., and Foster, W., "Analytical Methods for Predicting Grain Regression in Tactical Solid-Rocket Motors," *Journal of Spacecraft and Rockets*, Vol. 41, No. 4, 2004, pp. 689–693.

[7] Hartfield, R., Jenkens, R., Burkhalter, J., and Foster, W., "A Review of Analytical Methods for Solid Rocket Motor Grain Analysis," AIAA Paper 2003-4506, July 2003.

[8] Greatrix, D. R., "Internal Ballistic Model for Spinning Star-Grain Motors," *Journal of Propulsion and Power*, Vol. 12, No. 3, 1996, pp. 612–614.

[9] Willcox, M. A., Brewster, M. Q., Tang, K. C., and Stewart, D. S., "Solid Rocket Motor Internal Ballistics Simulation Using Three Dimensional Grain Burnback," *Journal of Propulsion and Power* (to be published).

[10] Blomshield, F. S., "Pulsed Motor Firings," NAWCWD TP 8444, China Lake, CA, March 2000.

[11] French, J. C., "Analytic Evaluation of a Tangential Mode Instability in a Solid Rocket Motor," AIAA Paper 2000-3698, July 2000.

S. Son
Associate Editor